Environmental Technology & Innovation 31 (2023) 103209

Contents lists available at ScienceDirect

Environmental Technology & Innovation

journal homepage: www.elsevier.com/locate/eti

Equilibrium study of benzene, toluene, ethylbenzene, and xylene (BTEX) from gas streams by black pine cones-derived activated carbon

Kaan Isinkaralar [a,*], Aydin Turkyilmaz [a], Sanaz Lakestani [b]

[a] Department of Environmental Engineering, Faculty of Engineering and Architecture, Kastamonu University, 37150, Kastamonu, Türkiye

[b] Scientific Industrial and Technological Application and Research Center, Bolu Abant İzzet Baysal University, 14280, Bolu, Türkiye

ARTICLE INFO

Article history:
Received 3 March 2023
Received in revised form 1 May 2023
Accepted 11 May 2023
Available online 18 May 2023

Keywords:
Biomass conversion
Carbonaceous material
Chemical activation
Surface functionalization
VOC capture

ABSTRACT

Considering environmental emissions, benzene, toluene, ethylbenzene, and xylene (BTEX) are widely used as raw materials in industrial processes. They also affect humans via inhalation, which must be reduced due to their toxicity before further operation. Notably, the leading technologies have tried to remove BTEX emissions with several methods. Continuous innovation of adsorbents is constantly developing in the adsorption mechanism, which has been developed based on waste biomass. *Pinus nigra* cones is a lignocellulosic raw material that is fast-growing on various soils and found abundant in nature as a precursor. It may be cheaply found available from some natural product vendors. It was used to prepare activated carbon by chemical activation with phosphoric acid (H_3PO_4), potassium hydroxide (KOH), sulfuric acid (H_2SO_4), lithium hydroxide (LiOH), zinc chloride ($ZnCl_2$), sodium hydroxide (NaOH) as the activating agents between at 550–850 °C for 2 h. Fourier transforms infrared spectrometer (FT-IR), thermogravimetric analyzer (TGA), scanning electron microscopy (SEM), and N_2 gas adsorption–desorption analyzer were used for KAS-ACs characterization. The high BTEX adsorption capacities by $ZnCl_2$ activated carbons were slightly higher than (S_{BET}: 1849 m^2/g for KAS-AC_{91}, and V_{total}: 0.44 cm^3/g) others. ANOVA results show a high correlation for the KAS-ACs production with $ZnCl_2$, and there was a statistically significant difference between the mean of V_{micro} (cm^3/g) with activation temperatures p-values<0.05. The removal capacities at 5 μg/L have been done to evaluate using Tenax TA tubes were 92, 96, 88, and 94.08% for benzene, toluene, ethylbenzene, and xylene, respectively. The maximum adsorption capacity for benzene, toluene, ethylbenzene, and xylene onto the KAS-AC_{91} in the following order: Xylenes (181 μg/g) > Toluene (206 μg/g) > Benzene (171 μg/g) > Ethylbenzene (201 μg/g). This suggests that the KAS-AC_{91} is an efficient BTEX adsorbent and represents a promising attempt to enhance BTEX adsorption in indoor air quality.

1. Introduction

BTEX (benzene, toluene, ethylbenzene, and xylene) are known to be volatile and flammable compounds widely distributed indoors. These compounds have generated a lot of air pollution, which is identified as a significantly persistent

* Corresponding author.
E-mail address: kisinkaralar@kastamonu.edu.tr (K. Isinkaralar).

https://doi.org/10.1016/j.eti.2023.103209

pollutant due to their solubility (Yang et al., 2019; Atamaleki et al., 2021). Through a literature review, BTEX emission increases in consumption levels emitted from transportation (Rivett et al., 2011), urbanization (Miller et al., 2012; Isinkaralar and Varol, 2023), production with chemical additives (Gaurh and Pramanik, 2018), oil refinery, silage (Hafner et al., 2013), e-waste recycling (Liu et al., 2022), various cooking styles (Wang et al., 2018a,b), smoking (Jafari et al., 2020), new furniture (Pei et al., 2016), and paints materials (Liu et al., 2014). It has been described and assessed the BTEX concentrations that it occurs many diseases and adverse health conditions due to their toxic and carcinogenic features (Jia et al., 2012; Rafiee et al., 2019). Widespread use rises considerably in the environment where significant BTEX emissions have raised concerns and possible generation of secondary organic aerosols and ozone formation in the atmosphere (An et al., 2014; Lim et al., 2014; Paris et al., 2020). For this reason, ambient BTEX removal is essential for public health protection and reactivity each other, and efforts to increase removal efficiency have gained momentum from indoor air quality (Laokiat et al., 2012).

BTEX is one of the most released gaseous pollutants in many household products from fugitive emissions. To restrain the required further increase in their emission, few investigations focused on the several control and capture techniques have been developed to remove BTEX by photocatalytic oxidation and degradation (Korologos et al., 2011; Liang et al., 2022), adsorption (Healy et al., 2019; Ouzzine et al., 2019; Isinkaralar, 2022a,b), absorption (Kong et al., 2018; Pontes-López et al., 2020), bio-filtration (Abdo and Huynh, 2021; Nayyeri et al., 2022), membrane filtration (Torasso et al., 2022), incineration (Ahamed et al., 2021), and combustion (Cheng et al., 2013). Among reviewed literature, the gas adsorption technique is one of the most used methods because of the reusability of materials and its high efficiency (Morris et al., 2013; Shi et al., 2020; Isinkaralar et al., 2022a). Accordingly, the BTEX adsorption capacity increases with the specific surface area, pore volume, surface functional groups, and especially with the increase of micropore volume (Isinkaralar and Turkyilmaz, 2022). Although various adsorbents are used in many studies, it is known that the frequently preferred activated carbons (ACs) are produced from multiple raw materials, indicating an increasing demand for waste biomass. Although methodologies for removing BTEX from the aquatic environment are commonly performed with ACs, it is seen that BTEX removal in the gas phase is not familiar.

The ACs are produced from several carbon materials from waste biomass (Mahamad et al., 2015; Zubrik et al., 2017; Mistar et al., 2020; Serafin et al., 2021; Isinkaralar et al., 2022b). It is an abundant and renewable green raw material that can be converted into valuable materials and energy. On this basis, the idea of using *Pinus nigra* cones is quite innovative and sustainable as a precursor. *Pinus nigra* J. F. Arnold is an evergreen forest tree that can grow up to 50 m and is one of the most commonly planted tree species (De Schrijver et al., 2008). Its bark is deeply fissured from a young age, thickens on older stems, and turns from dark gray-black to whitish (Martín-Benito et al., 2008). The female cones are bright, straw yellow, brown, and ovoid-conical. It is symmetrical and has a very short stem. The shield is prominent, the belly is dark, and a small thorn is in the middle. Cone length varies between 3–12 cm; as age progresses, it becomes waste biomass. Although the immature *P. nigra* cones are sold in small amounts, they cannot be evaluated economically. However, while the cones need to mature for seed production, they contribute to forest fires and are planted on erosion slopes and abandoned agricultural land (Mikulová et al., 2019). For this reason, they are collected periodically during the summer, derived from the large amount of waste biomass used for the ACs. They are produced from carbonization and are interesting due to their large sample. Consequently, a significant amount of low-cost bio-based materials should be made to mitigate the BTEX remediation from the air environment.

Based on the authors' knowledge, this is a practical study that analyses the utilization of multi-component mixed for capturing BTEX components while simultaneously checking the adsorption behavior of selected KAS-ACs as filter material. Therefore, the main aims of this experimental study are to identify three complementary strategies:

1. The preparation of carbon-based adsorbent using *P. nigra* cones was investigated as an ideal feedstock for BTEX removal because there is no reported research on the utilization of *P. nigra* cones biomass (PNCB) as a precursor of ACs (KAS-ACs).
2. The one hotspot for BTEX efficiencies is excellent physicochemical properties because of its varying production process, such as carbonization and impregnation activating agents.
3. The investigation is needed to understand spearheading research as no reported literature studies on waste biomass synthesized activated carbon for compressibility behavior and properties of BTEX capture.

2. Materials and methods

2.1. Chemicals and biomass

Black pine (scientific name *Pinus nigra*) cones were procured from the regional forest in Kastamonu, Türkiye, and were denoted as PNCB. Sulfuric acid (H_2SO_4), phosphoric acid (H_3PO_4), potassium hydroxide (KOH), lithium hydroxide (LiOH), sodium hydroxide (NaOH), zinc chloride ($ZnCl_2$), benzene (C_6H_6), toluene (C_7H_8), ethylbenzene (C_8H_{10}) and xylene (C_8H_{10}) were used analytical grade (over 99%). Tenax TA (60/80 mesh) tubes were purchased from Sigma-Aldrich and Supelco (Bellefonte, PA, USA). BTEX stock solution was reached by adding the required volume of distilled water to generate solutions of adsorbate with several initial concentrations from 5 to 360 μg/L.

2.2. Preparation of KAS-ACs

KAS-ACs were synthesized using as follows: (i) PNCB were cut into small pieces, then solid samples were washed many times with distilled water to remove impurities and contaminants; (ii) dried before going further operation in an oven at 105 °C for 24 h; (iii) PNCB were ground and sieved range of 250–500 μm for standardization regular particle size before use and weighed to 20 g for each sample, (iv) 100 mL of 20, 40, and 60% (w/v) KOH were added to 20 g of PNCB powder with impregnation ratio 1.00: 0.50, 1.00, 2.00, 3.00 and 5.00, i.e., 20 g biomass and 20 g KOH in 100 mL distilled water and mixed thoroughly; (v) the mixture was left for 24 h and then dried at 105 °C for 5 h, and thermal treatment of samples by pyrolysis process was applied using a homemade designed stainless fixed-bed reactor equipped with a tubular furnace at between 550, 650, 750, 850, and 950 °C (heating rate of 10 °C/min) and held for 120 min under continuous flowing nitrogen (N_2) with a flow of 80 mL/min; (vi) Then ACs produced were labeled as KAS-ACs and washed with powerful mixing using boiling deionized water to eliminate acid–base (adjusted to pH:7.00) and allowed to dry at 100 °C for 20 h; (vii) the same way was repeated using LiOH, NaOH, $ZnCl_2$, H_2SO_4, and H_3PO_4. The KAS-ACs were stored for further use in physicochemical characterizations and BTEX application. The final products were named in a range from KAS-AC_1 to KAS-AC_{120} for the BTEX adsorption.

2.3. Characterization of KAS-ACs

The physical properties of the KAS-ACs were impregnated with H_3PO_4, KOH, H_2SO_4, LiOH, $ZnCl_2$, and NaOH, respectively. Their morphologies and surface particulars were studied with a scanning electron microscope (SEM, by FEI Quanta FEG 250) at 10 kV and 4500 x. Fourier transforms infrared spectrometer (FT-IR) was used in the content and type of functional groups on the KAS-ACs. During Perkin Elmer FT-IR spectroscopy analysis, a KBr tablet was performed in the optimum spectral scanning wavenumber range of 400–4000 cm^{-1}, scanning speed of 0.2 cm/s and resolution of 0.06 cm^{-1}. The elemental analyses determined the elemental contents of C, H, N, and O by the elemental analyzer (Eurovector brand by EA3000-Single). The specific surface area (S_{BET}), volume of BET/total and micropore and pore size distribution were found using Brunauer–Emmett–Teller (BET) and t-plot method were utilized to calculation their numeric values by the Quantachrome surface area analyzer device. The volume of KAS-ACs was determined based on the N_2-adsorbed's amount ($P/P0 = 0.95$). The adsorption and desorption isotherms were measured until 1.00 atm at 77 K with high purity N_2. A thermal gravimetric analyzer (TGA) was used for the contents of surface groups from 50 to 850 °C at 20 °C/min under N_2 flow of 100 mL/min.

2.4. Batch adsorption

The adsorption of BTEX by KAS-ACs was investigated in a batch reactor in Fig. 1. The experiments were performed in steady-state conditions to verify adsorption conditions, which can be prepared at the following operation conditions: KAS-ACs dosage of 0.25 g, initial concentration ranging from 5–360 μg/L, and constant temperature of 23 °C. The 0.25 g KAS-ACs were placed and positioned in the center of the batch reactor, which executed an adsorption mechanism to extend contact time up to 100 min. After the addition of KAS-ACs, the quantity of BTEX adsorbed capacity at equilibrium was calculated by use of Eq. (1):

$$q_{(mg/g)} = \left(\frac{F \times C_0 \times 10^{-9}}{W}\right)\left[\left(\frac{C_i}{C_0} \times t_s\right) - \left(\int_0^{t_s} \frac{C_i}{C_0} d_t\right)\right] \quad (1)$$

where C_i (μg/L) and C_o (μg/L) denote inlet and outlet BTEX concentration at equilibrium concentration, F and W represent a feed flow rate (mL/min), and adsorbent weight (g).

Examining the adsorption rate and mechanism for the removal of volatile compounds onto the KAS-ACs is essential to develop a new solid-gas phase equilibrium model based on experimental data.

Tenax TA® sorbent tube (60/80 mesh and 200 mg) was used to adsorb target compounds, mainly due to the displacement of diffused molecules. The total number of tubes sampled was 120 Tenax TA tubes experiments. The BTEX samples were collected into a Tenax TA® sorbent tube connected to an air collector pump (SKC Model 220, USA) with a 50 mL/min flow rate. Pump rotameters calibrated the air pump with an accuracy of ±1%. Collected BTEX samples in Tenax TA® tubes were further evaluated by gas chromatography/mass spectrometric (GC/MS, brand by Thermo Scientific Trace 1300) and mass detector with a capillary column (TG-624; 30.0 m×0.25 mm ×1.4 μm film thickness, Thermo Scientific ISQ QD) was connected to thermal desorption unit (TD, ultra-high purity helium gas at a flow rate of 40 mL/min) Unity-1 and Ultra Series 2 (Markes International, UK) for determine the amount of BTEX. After sampling, each Tenax tube was tightly sealed, wrapped by aluminum foil, and stored at −20 °C for 2 weeks. Then, GC/MS rapidly prepared for the selective ion monitoring (SIM) mode for scan and identify BTEX compounds with the MSD operated at electron impact (EI) ionization at 70 eV and maintained at 230 °C. Also, the desorption efficiency of the BTEX from TD scale was >98%. The method detection limit (MDL) for the BTEX compounds ranged from 0.009 to 0.165 ppbv, and the measurement precisions for the analysis of eight replicates of standard samples at 2 ppbv were ≤5%.

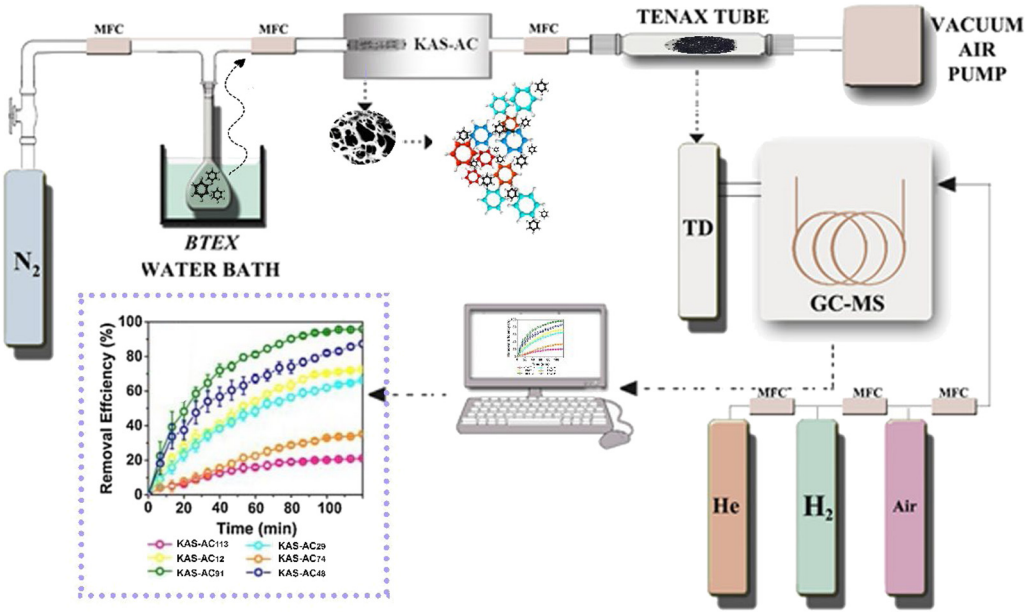

Fig. 1. Schematic illustration of BTEX removal procedure from gasification system.

2.5. Statistical methods

The statistical calculations were performed using Statgraphics Centurion XV software (Statpoint Technologies Inc., Warrenton, VA, USA). Descriptive statistics (mean and standard deviation) initially investigated the continuous bacteria concentration data. Then, a one-way analysis of variance (ANOVA) was performed between the surfaces, activating agents, and temperatures. A 95% confidence interval was used to evaluate the *p*-value to inspect the significance of the model. The multiple comparison procedures were used to determine which means differed significantly from others. Fisher's exact test, the least significant difference (LSD) procedure, is currently used to discriminate among the means. The mechanism associated with the 5% risk of calling each pair of means significantly different when the actual difference equals 0. Multiple range tests were selected to determine which means are quite different from others. The activating agent for the BET surface area was applied, and the least statistically significant difference (LSD) was observed between the groups.

3. Results and discussion

3.1. Instrumental characterization of KAS-AC

As significant the physicochemical structures of KAS-ACs, pore development, weight loss, and containing components on the functional groups were investigated to show the different physicochemical functionality between the combination of chemical agents. The KAS-ACs surface area and porosity were considered to ascertain discrepancies with H_3PO_4, KOH, H_2SO_4, LiOH, $ZnCl_2$, and NaOH during impregnation. The agglomerated surface in the KAS-ACs was recorded with SEM, FT-IR, and TGA, respectively. The isotherms were classified by IUPAC, the pore structure accompanied the N_2 adsorption–desorption at 77 K in the pore structure parameters (micro, meso, macro size), and all of the KAS-ACs isotherms are typical type I by the non-local density functional theory (NLDFT) in Fig. 2 These results provide further that the combination of the microporous–mesoporous structure of KAS-ACs is formed stably and associated with very low relative pressures ($P/P_0 < 0.4$) (Cazetta et al., 2011). The mesoporous structure comprises visible until 0.6 relative pressure (Peng et al., 2014). Large and well-developed pores for each activating the impregnated precursor were apparently approved on the surface of KAS-AC_{12}, KAS-AC_{29}, KAS-AC_{48}, KAS-AC_{74}, KAS-AC_{91}, and KAS-AC_{113} would be the primary factor for enhancing the BTEX adsorption capacity.

Table 1 shows the elemental analysis of PNCB and KAS-ACs. The condition before the activation of PNCB demonstrates as follows: C (47.07%), H (5.58%), N (0.65%), O (17.22%), and ash (29.48%), however after activation was obtained to enrich the KAS-ACs s as follows: C (54.35 to 74.32%), H (2.03 to 3.30%), N (0.11 to 1.78%), O (18.53 to 30.92%), and ash (2.56 to 10.68%). The results of KAS-ACs show the main reason C (%) content indicates a successful conversion from PNCB; the O (%) content is higher than C, H, and N due to the formation of groups. They were appointed in structures in which unwanted compounds might happen and replaced by several responsible groups. Lignocellulosic content like PNCB is a high-grade carbon precursor for factoring ACs due to its high C content of more than >45% (Ahmedna et al., 2000)

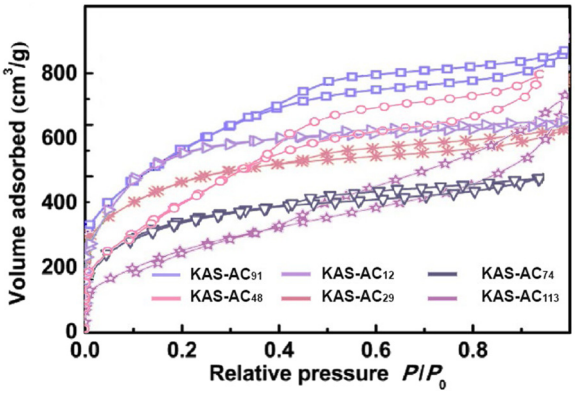

Fig. 2. Adsorption/desorption isotherms (N_2 at 77 K) of KAS-ACs.

Table 1
The elemental compositions and ash content of PNCB and KAS-ACs.

Elemental analysis (%)	PNCB	KAS-AC_{12}	KAS-AC_{29}	KAS-AC_{48}	KAS-AC_{74}	KAS-AC_{91}	KAS-AC_{113}
C	47.07	70.02	66.45	73.81	58.19	74.32	54.35
H	5.58	3.02	3.49	2.61	2.88	2.03	3.30
O	17.22	18.53	19.61	20.91	20.82	18.98	30.92
N	0.65	0.39	1.78	0.11	0.91	0.46	0.75
Ash	29.48	8.04	8.67	2.56	17.2	4.21	10.68

Fig. 3 shows SEM images of PNCB, KAS-AC_{12}, KAS-AC_{29}, KAS-AC_{48}, KAS-AC_{74}, KAS-AC_{91}, and KAS-AC_{113} in the porosity characterization before the activation process and after loading the activating agents. A similar morphological structure has been previously found for other biomaterials, such as corn stalks (Zubrik et al., 2017) and *Gleditsia riacanthos* L. (Isinkaralar, 2023a). The changes appear remarkable differences as heterogeneous voids and cracks of surface and pores. The morphology structure for KAS-ACs was performed according to a previous study by Kang et al. (2015). The development in the morphology of the structure has emerged, which can be regarded nearly at the medium level. It has been controlled that the design diversities result from hetero chemical agents used in each of them. The idea of the irregularly shaped pores suggests that the KAS-ACs surface with increase the diffusion resistance of BTEX molecules; thus, sorption equilibrium will have a higher sorption capacity.

Fig. 4 shows FT-IR spectral analysis; besides carbon atoms, it examined changes in functional groups (carboxyl, carboxylic anhydride, phenol, lactone, etc.) of PNCB, KAS-AC_{12}, KAS-AC_{29}, KAS-AC_{48}, KAS-AC_{74}, KAS-AC_{91}, and KAS-AC_{113}, respectively. The FT-IR spectrums represent carbon metrix by heteroatoms such as H_2, N_2, and O_2, forming surface chemistry by the acidity and basicity of KAS-ACs surface (Kumar and Jena, 2016). The bands at 3487 cm^{-1} correspond to the stretching vibration of the O–H bond of hydroxyl groups (González-García et al., 2013). The other peaks concentrated between 2811 and 3100 cm^{-1} could be dedicated to the asymmetric stretching of C–H, and the small band at 2420 cm^{-1} argues the stretching of C≡C bond. The prominent peak at 1420–1590 cm^{-1} exhibits C=C bonds from the aromatic ring (Cao et al., 2016; Mistar et al., 2020), and 1243 cm^{-1} refers to C–O–C bond stretching. Typically, the other firm peaks at 821 and 1079 cm^{-1}, providing C–H derivatives and C–O bonds stretching between amino groups and chloride compounds (Ovchinnikov et al., 2016). It is close to the peak values taken by Najafi et al. (2011), who state that they correspond to the stretching vibration of the (C-S)-others bond at 614 cm^{-1}. The FT-IR spectrum of KAS-AC_{12}, KAS-AC_{29}, KAS-AC_{48}, KAS-AC_{74}, KAS-AC_{91}, and KAS-AC_{113} depictures notable change at 1400–1700 cm^{-1} with subtle amendments in the band's intensity.

Fig. 5 represents the carbonation temperature; the TGA thermograms of the KAS-ACs were analyzed of the PNCB, KAS-AC_{12}, KAS-AC_{29}, KAS-AC_{48}, KAS-AC_{74}, KAS-AC_{91}, and KAS-AC_{113}, respectively. The weight loss curves show three primary decompositions can be observed at 70 °C as the first step, 358–470 °C as the second step, and 610–726 °C as the third step during the process of pyrolysis. A systematic decrease and rate loss were observed, with a weight loss from 10.7 to 26.8% due to the different volatility of compounds. Until 270 °C, weight loss pertains to interlayer water and surface adsorption evaporation; however, 410–830 °C is essential for KAS-ACs combustion (Liu et al., 2016). This may be attributed to the remarkable curve between KAS-AC_{12} and KAS-AC_{113} which makes the H_3PO_4 and LiOH activation more pronounced and affects the main surface's fraction.

Table 2 shows the effect of H_2SO_4, H_3PO_4, LiOH, KOH, NaOH, and $ZnCl_2$ on production efficiency. The maximum concentration measured in BET surface area was 1783 cm^3/g at 650 °C for H_2SO_4, 1503 cm^3/g for H_3PO_4, 1390 cm^3/g for KOH, 502 cm^3/g for LiOH, 873 cm^3/g for NaOH, and 1849 cm^3/g for $ZnCl_2$ at 750 °C. The maximum value was determined at 750 °C in all experiments.

Various amounts of the presence of BTEX have been stated in many studies to be dangerous for public health and atmospheric chemistry (Rad et al., 2014; Tamrakar et al., 2022). Based on these, studies have been conducted to reduce

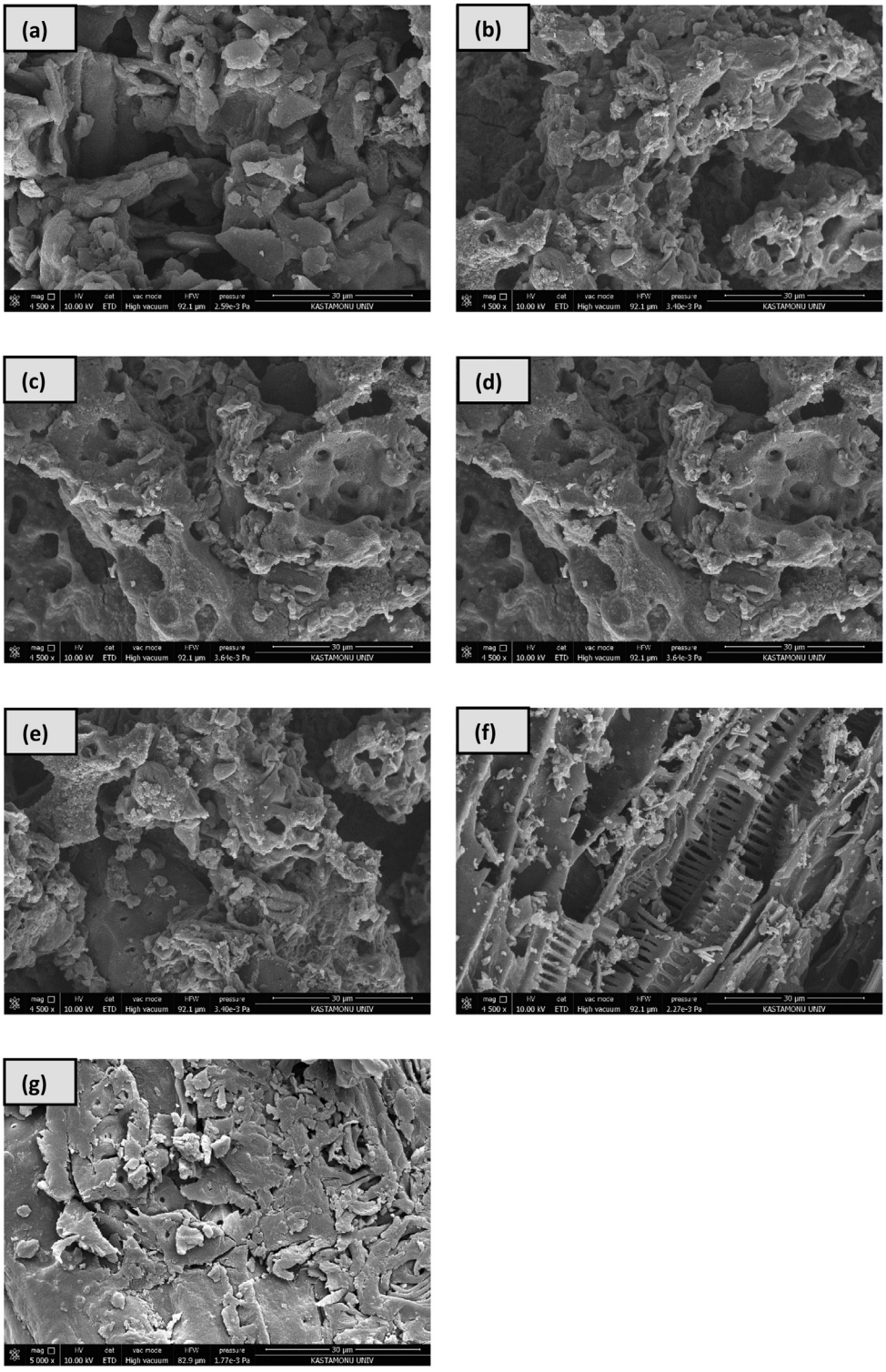

Fig. 3. SEM images of (a) PNCB; (b) KAS-AC_{12}, (c) KAS-AC_{29}, (d) KAS-AC_{48}, (e) KAS-AC_{74}, (f) KAS-AC_{91}, and (g) KAS-AC_{113}.

BTEX concentrations in the indoor environment due to its high reactivity (Latif et al., 2019; Alenezi and Aldaihan, 2019; Fang et al., 2019). Due to the continuity of the oscillations of BTEX, which is eliminated by various methods, in the existing indoor air, it is vital to find a continuous process, not one-time removal or one-time treatment. It is a prevalent

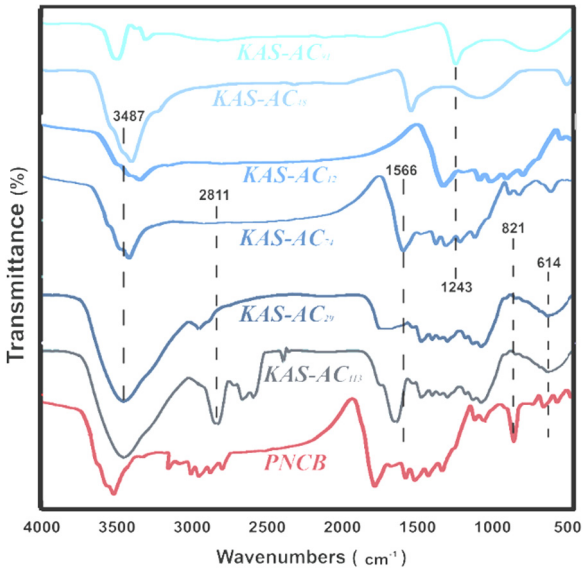

Fig. 4. FT-IR spectra of PNCB and selected KAS-ACs.

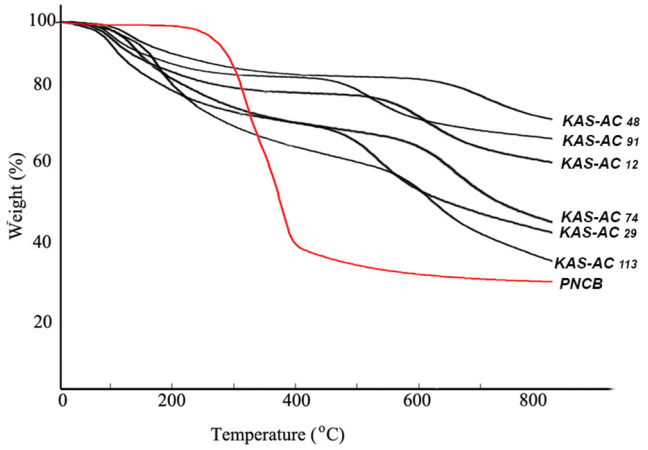

Fig. 5. Thermal treatment curves of PNCB and selected KAS-ACs.

Table 2
The total surface area (m^3/g) of KAS-ACs.

Activating agent	*N	Mean ± SD	Minimum	Maximum	Adsorbent ID
H_3PO_4	120	728.10 ± 435.56	177	1503	KAS-AC_{12}
KOH	120	694.60 ± 390.73	103	1393	KAS-AC_{29}
H_2SO_4	120	898.90 ± 450.95	288	1783	KAS-AC_{48}
NaOH	120	466.60 ± 232.416	33	873	KAS-AC_{74}
$ZnCl_2$	120	943.10 ± 480.964	202	1849	KAS-AC_{91}
LiOH	120	189.55 ± 155.335	11	502	KAS-AC_{113}

*N: Number of samples.

issue that the materials used in the indoor environment invite diseases with increased BTEX emission via intensive chemical reactions at room temperatures (even at low concentrations). The literature has reported adsorption with ACs technologies, which is continuously used among the methods and is cheap and easy to use (Policicchio et al., 2015; Nandanwar et al., 2016). Raw material can be plentiful and free, put into various forms if desired, and allows multiple gas adsorption, which seems quite reasonable (Pallarés et al., 2018; Laskar et al., 2019). Although much investigation has been carried out in this context, BTEX removal is a scorching topic because it is very up-to-date, and its removal has not been done perfectly yet (Li et al., 2020; El Mohajir et al., 2021).

Table 3
Comparison of V_{micro} (cm^3/g) by activating agents.

Activating agent	*N	Mean ± SD	Minimum	Maximum
H_2SO_4	120	0.29 ± 0.17	0.04	0.71
H_3PO_4	120	0.27 ± 0.10	0.11	0.50
KOH	120	0.27 ± 0.05	0.16	0.34
LiOH	120	0.10 ± 0.02	0.06	0.13
NaOH	120	0.19 ± 0.05	0.10	0.34
$ZnCl_2$	120	0.22 ± 0.10	0.10	0.44

*N: Number of samples.

Table 4
Multiple range tests for V_{micro} (cm^3/g) by activating agent.

Level	Count	Mean	Homogeneous groups
LiOH	120	189.55	A
NaOH	120	466.6	B
KOH	120	694.6	BC
H_3PO_4	120	728.1	CD
H_2SO_4	120	898.9	CD
$ZnCl_2$	120	943.1	D

Table 3 shows the results for the maximum V_{micro} values were 0.71 cm^3/g at 750 °C for H_2SO_4, 0.50 cm^3/g at 750 °C for H_3PO_4, 0.34 cm^3/g at 750 °C for KOH, 0.13 cm^3/g at 850 °C for LiOH, 0.34 cm^3/g at 850 °C for NaOH, and 0.44 cm^3/g at 850 °C for $ZnCl_2$. The highest amount was determined at 750 °C on the micropore surface for all agents. By comparison, it is found that several ACs production for gas adsorption has been reported in laboratory-scale experiments via gas-to-particle transformation processes (Ogungbenro et al., 2018; Guo et al., 2020; Zhou et al., 2020; Isinkaralar, 2023b). It is well recognized that biomass source remarkably affects the specification of the outcome ACs. Although our focus here is on BTEX removal, the overall objective of steady-state conditions of BTEX indoors was to better describe each molecule's behavior in the adsorption. The BTEX elimination decreased in the order toluene > xylene > benzene > ethylbenzene by KAS-AC_{91}.

In order to better comprehend the V_{micro} (cm^3/g) of the KAS-ACs pore distribution at the activation conditions was a statistically significant difference between the mean of V_{micro} (cm^3/g) with activation temperatures ($p < 0.05$). However, it demonstrates no statistically significant difference. A multiple comparison procedure is to determine which means significantly differ from others. An asterisk has been placed next to 9 pairs. These pairs showed statistically significant differences at the 95.0% confidence level. Four homogeneous groups are identified using columns of x's within each column. The levels containing x's form a group of means within which no statistically significant differences exist (see Table 4).

3.2. Effect of experimental variables

The effect of initial compounds concentrations from 5 to 360 μg/L and contact time (until 100 min) was maintained through the adsorption capacity of KAS-ACs in Fig. 6. The efficiency obtained in the first 5 min of the experiments was compared with the yield at the end, demonstrating a drastic increase in the products found to be close. Against this baseline, benzene, toluene, ethylbenzene, and xylene had the highest yields at 5 μg/L and the lowest at 360 μg/L. It is expected that at the low KAS-ACs usage, the dispersion of BTEX particles in the vapor is better; that is, all of the active sites on the KAS-ACs surface are exactly apparent, which may expedite the approachability of BTEX molecules to a large number of the KAS-ACs active sites. Accordingly, the adsorption on the KAS-ACs surface is attained to a saturated point, exhibiting a high elimination capacity by imparting functionalities to the KAS-ACs. Despite the specifications mentioned above, at higher KAS-ACs loading, the accessibility of active sites with higher energy declines. An enormous amount of the active sites with lower energy is occupied, decreasing the adsorption mechanism. Therefore, 0.25 g of KAS-ACs was selected as the proper fit for the rest of the test.

Further along, the capturing with 0.25 g KAS-AC_{91}, the highest yields in benzene, toluene, ethylbenzene, and xylene were 92, 96, 88, and 94.08%, while the lowest results were 50, 56.94, 47.25, and 57%, respectively. To support the above statement, Shen and Zhang (2019) synthesized an adsorbent from the silica-rich rice husk, and its maximum S_{BET} and V_{micro} were found to be 1818 m^2/g and 0.84 cm^3/g using the KOH as RH char-3. 300 ppm toluene and 60 ppm phenol within the sorption column were performed gas-phase by the online GC-FID analysis. The RH char-3 showed excellent toluene capacity with 263.6 mg/g; however, the phenol adsorption capacity was relatively low at 6.53 mg/g. Similarly, in our study, depending on the volatility of the molecules and the initial concentration, there are variations in the adsorption capacity. They produced hydrochars from hickory wood and peanut hull by KOH and H_3PO_4. They compared the highest surface area that H_3PO_4 activation was obtained at 1436 and 1091 m^2/g as bigger than KOH activation at 222 and 571 m^2/g (Zhang et al., 2019). Also, they reported acetone and cyclohexane adsorption capacities increased significantly to 50.57–159.66 mg/g.

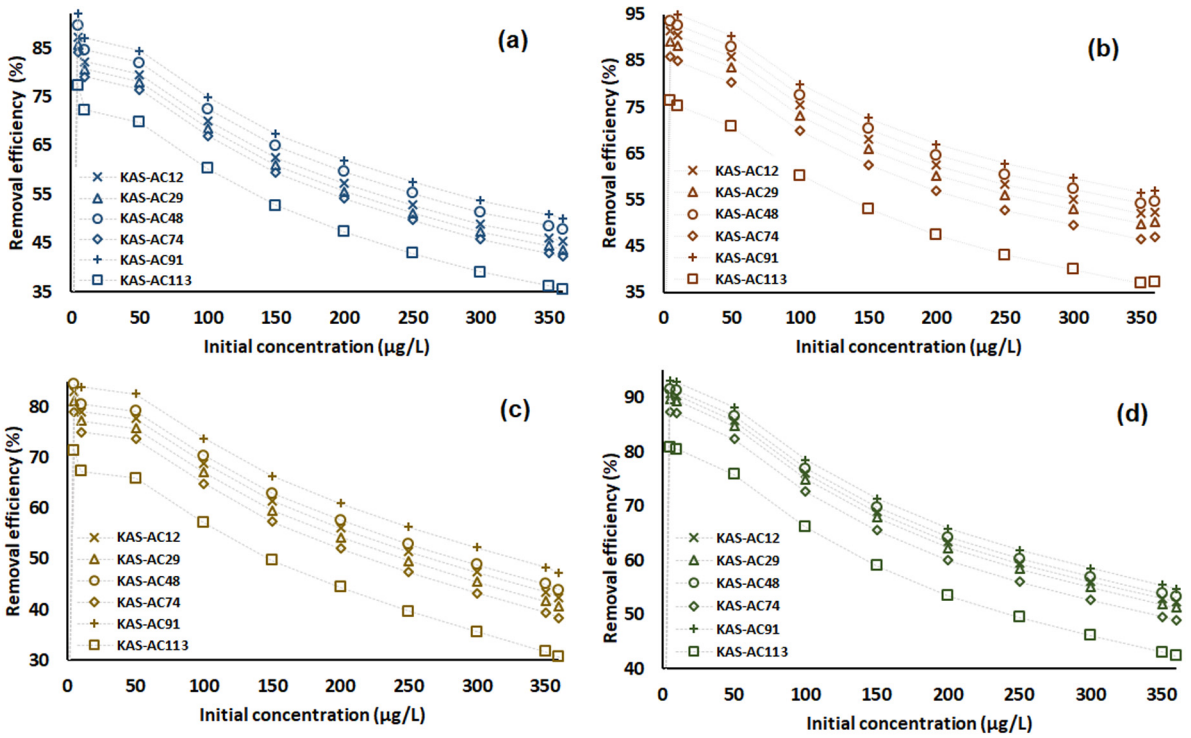

Fig. 6. The removal efficiency plots for the adsorption of (a): benzene; (b): toluene; (c): ethylbenzene; and (d): xylene onto KAS-ACs.

This indicates that the mobility of benzene has a relatively low reactivity compared to the dynamism of ethylbenzene and xylenes; it can be transported to another adsorbent without degradation in a lower amount than others (Bauri et al., 2016; Dehghani et al., 2018). A similar phenomenon of lignocellulosic adsorbents having superior performance toward BTEX adsorption was observed in this study. The carbon-based support, KAS-AC_{91} could propose an assertive behavior for a potential industrial gas application.

Adsorption capacities were not checked for each adsorbent. The essential reason for this is the high number of KAS-AC_{91}, which has high efficiency and was chosen after the efficiency calculation in Fig. 7. The highest adsorption capacity for each substance was found during 100 min. As the concentration increased in the first 10 min of contact time, the trend of the increase was due to availability in the occupancy and vacant sites of pores. But the amount needed to reach equilibrium was kept constant to be 0.25 g. Among these compounds, the constant amount of adsorbent saturation rate can be easily seen after 20 min and then at a slow speed. The rapid adsorption at the initial stage until 20 min was most presumably due to the raised concentration gradient between the BTEX vapor, and that depends, fundamentally, on the KAS-AC_{91} as there could be an increased amount of empty regions attainable in the beginning. In contrast, the concluded plateau after 30 min growth tendency paused when a case of the equilibrium rate of BTEX molecules on the KAS-AC_{91}. Its adsorption capacity increases with increasing initial BTEX concentration because the initial concentration provides a significant driving force to overcome all mass transfer resistance. Similar results for the removal of VOCs have been reported by many researchers (Baur et al., 2015; Sui et al., 2017; Stähelin et al., 2018; Wang et al., 2018b). Over time, the coverage of BTEX molecules on the surface of the KAS-AC_{91} increased. The enhancement in BTEX concentration at the outlet flow was remarked to the reduction in the sticking possibility of BTEX as more active sites were occupied in KAS-AC_{91}.

For illustrative purposes, much more toluene and xylene were sorbed onto KAS-AC_{91} than KAS-ACs, which the molecular structure, such as the molecular weight and boiling point, may cause. The molecular weight of volatiles can impact their adsorption onto an adsorbent. It was found that the diffusion coefficients of xylene and toluene were significantly higher than benzene molecules. The present amount findings are in line with the gas adsorption studies that adsorbed amount 206 µg/g for xylene had a higher than 181 µg/g for benzene, which may be why xylene had an excellent capacity than benzene. The boiling points of benzene (80.1 °C) has lower than that of lower boiling point toluene (110.6 °C) and xylene (138.4 °C), which may be caused by favorably adsorbed for their powerful intermolecular forces with the KAS-AC_{91}. According to initial concentration, many recent studies indicated that carbon-based derived from usually used biomass had BTEX adsorption capacity, which showed large scale mg/g. Also, similar results have been conducted on volatile adsorption by several adsorbents due to their strong affinity by different boiling points (Dobre et al., 2014; Giraudet et al., 2014; Shakeri et al., 2016; Verma et al., 2019; Isinkaralar and Meruyert, 2023). As argued by Ahmed

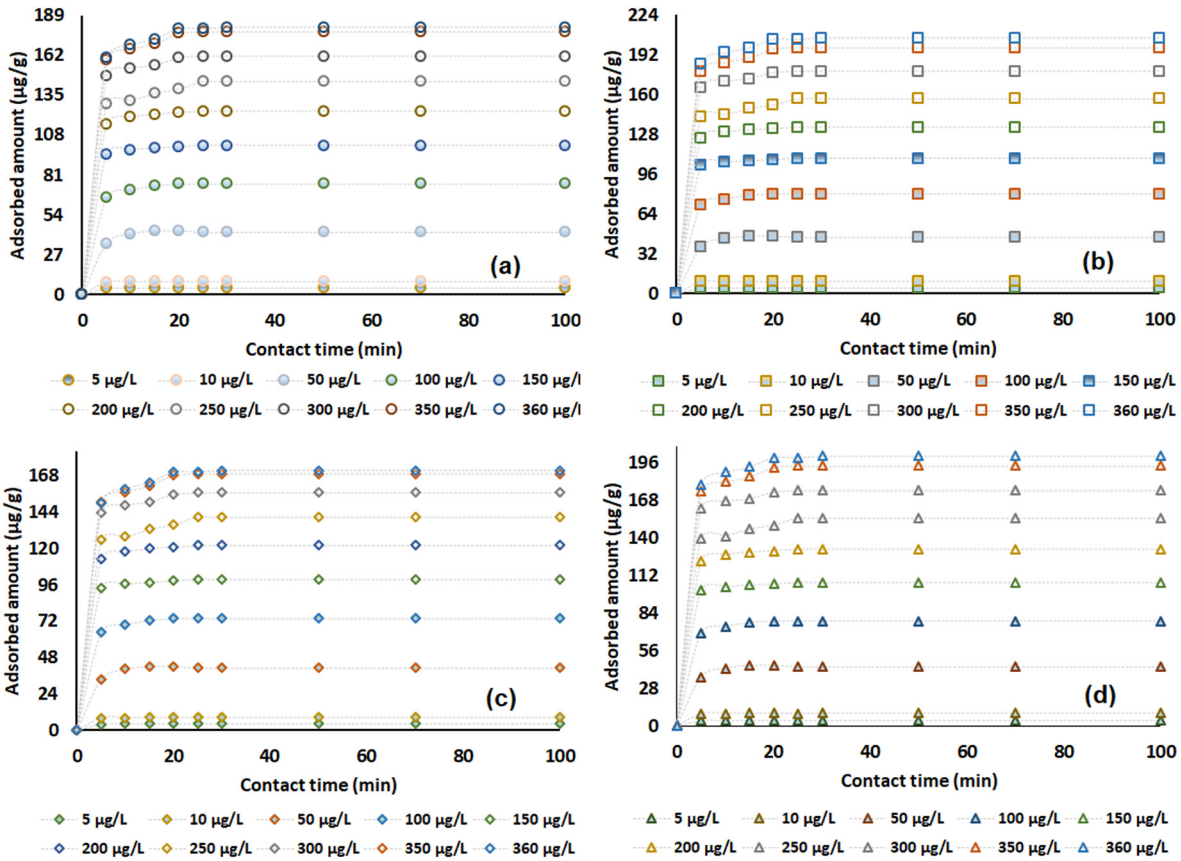

Fig. 7. Relationship between contact time and adsorption capacity (µg/g) of (a): benzene, (b): toluene, (c): ethylbenzene, and (d): xylene onto KAS-AC_{91}.

et al. (2019), there is also prepared several ACs derived from biomasses for adsorbing CO_2 gas; however, AC-2 was highly efficient at 39.70 kJ mol^{-1}. Meng et al. (2019) tried to eliminate VOCs with activated carbon fibers from Lignin alkali using KOH (LCFK) and selected toluene, methanol, and acetone for dynamic adsorption. They examined multi-component volatile adsorption onto LCFK and found that they are combined; fewer yields are obtained than the individual removal efficiencies. More recent arguments find that BTEX adsorption onto different adsorbents, and several researchers came to the same conclusion (Seifi et al., 2011; Konggidinata et al., 2017; Rahimpoor et al., 2021). The above results and adsorption as a dramatic method for VOCs recommend their possible execution in removing gas compounds. On the other hand, the adsorption mechanisms associated with removing benzene, toluene, ethylbenzene, and xylene using KAS-AC_{91} can involve their surface interactions that contribute to each molecule and the negative surface charge of the adsorbent. Furthermore, a detailed cost estimation would be beneficial to highlight the cost-effectiveness of this process, such as production, operation, and maintenance.

4. Conclusions

In summary, adsorption is considered the most promising technology due to its many advantages. The adsorption onto KAS-AC_{91} of benzene, toluene, ethylbenzene, and xylene (BTEX) in the gas phase was examined in a batch reactor. Consistent with the applied removal approach, the main conclusions acquired are on four criteria: (i) the KAS-AC_{91} was successfully prepared from *P. nigra* cones as agricultural waste by pyrolysis of is biomass with $ZnCl_2$-activation at 750 °C for 120 min, (ii) the physical and chemical characteristics of KAS-AC_{91} and PNCB were also analyzed, which would supply more adsorption zones for BTEX molecules, (iii) differences examined the BTEX adsorption process for initial BTEX concentrations, and contact time, (iv) gradually increased after penetration, the maximum capacity of benzene, toluene, ethylbenzene, and xylene were found as 181, 206, 171, and 206 µg/g for KAS-AC_{91}, respectively. Also, the contact time of BTEX on the adsorption was short (100 min) and is needed to try several temperatures and may extend to 300 min. Generally speaking, the BTEX adsorption shows the degradation pathways differ in details resulting from adsorption operating conditions onto KAS-AC_{91} due to its micropores playing a role in decreasing. Here we present the BTEX

findings argue that KAS-AC_{91}, with a low-cost, environmentally friendly production and high surface area, recommends the terseness of removing BTEX gases and successful operation with single-component sorption systems into the ambient air. The conclusions provide that KAS-AC_{91} could be evaluated as an effective, sustainable material for air pollutants. It can be easily used for future work from large-scale removal technology.

CRediT authorship contribution statement

Kaan Isinkaralar: Raw material collection, Methodology, Processing analysis, Project administration, Writing – original draft, Validation interpretation. **Aydin Turkyilmaz:** Conceptualization, Visualization, Resources, Writing – review & editing. **Sanaz Lakestani:** Conceptualization, Software, Writing – review & editing.

Declaration of competing interest

The authors declare that they have no known competing financial interests or personal relationships that could have appeared to influence the work reported in this paper.

Data availability

Data will be made available on request.

Acknowledgment

The authors are thankful to the Kastamonu University for the research facilities.

Funding

We would like to thank the financial support provided by the Kastamonu University Scientific Projects Research Office Project Number (KÜBAP01/2021-18) Kastamonu, Türkiye.

References

Abdo, P., Huynh, B.P., 2021. An experimental investigation of green wall bio-filter towards air temperature and humidity variation. J. Build. Eng. 39, 102244. http://dx.doi.org/10.1016/j.jobe.2021.102244.

Ahamed, A., Liang, L., Chan, W.P., Tan, P.C.K., Yip, N.T.X., Bobacka, J., Veksha, A., Yin, K., Lisak, G., 2021. In situ catalytic reforming of plastic pyrolysis vapors using MSW incineration ashes. Environ. Pollut. 276, 116681. http://dx.doi.org/10.1016/j.envpol.2021.116681.

Ahmed, M.B., Johir, M.A.H., Zhou, J.L., Ngo, H.H., Nghiem, L.D., Richardson, C., Moni, M.A., Bryant, M.R., 2019. Activated carbon preparation from biomass feedstock: clean production and carbon dioxide adsorption. J. Clean. Prod. 225, 405–413. http://dx.doi.org/10.1016/j.jclepro.2019.03.342.

Ahmedna, M., Marshall, W.E., Rao, R.M., 2000. Production of granular activated carbons from select agricultural by-products and evaluation of their physical, chemical and adsorption properties. Bioresour. Technol. 71 (2), 113–123. http://dx.doi.org/10.1016/S0960-8524(99)00070-X.

Alenezi, R.A., Aldaihan, N., 2019. Impact of fuel dispensing stations in the vicinity residential homes on the indoor and outdoor air quality. Int. J. Environ. Sci. Technol. 16 (6), 2783–2796. http://dx.doi.org/10.1007/s13762-018-1834-4.

An, T., Huang, Y., Li, G., He, Z., Chen, J., Zhang, C., 2014. Pollution profiles and health risk assessment of VOCs emitted during e-waste dismantling processes associated with different dismantling methods. Environ. Int. 73, 186–194. http://dx.doi.org/10.1016/j.envint.2014.07.019.

Atamaleki, A., Motesaddi Zarandi, S., Massoudinejad, M., Samimi, K., Fakhri, Y., Ghorbanian, M., Khaneghah, A.M., 2021. The effect of frying process on the emission of the volatile organic compounds and monocyclic aromatic group (BTEX). Int. J. Environ. Anal. Chem. 1–14. http://dx.doi.org/10.1080/03067319.2021.1950148.

Baur, G.B., Beswick, O., Spring, J., Yuranov, I., Kiwi-Minsker, L., 2015. Activated carbon fibers for efficient VOC removal from diluted streams: the role of surface functionalities. Adsorption 21, 255–264. http://dx.doi.org/10.1007/s10450-015-9667-7.

Bauri, N., Bauri, P., Kumar, K., Jain, V.K., 2016. Evaluation of seasonal variations in abundance of BTXE hydrocarbons and their ozone forming potential in ambient urban atmosphere of dehradun (India). Air Qual. Atmos. Health 9 (1), 95–106. http://dx.doi.org/10.1007/s11869-015-0313-z.

Cao, W., Cao, C., Guo, L., Jin, H., Dargusch, M., Bernhardt, D., Yao, X., 2016. Hydrogen production from supercritical water gasification of chicken manure. Int. J. Hydrogen Energy 41 (48), 22722–22731. http://dx.doi.org/10.1016/j.ijhydene.2016.09.031.

Cazetta, A.L., Vargas, A.M., Nogami, E.M., Kunita, M.H., Guilherme, M.R., Martins, A.C., Silav, T.L., Moraes, J.C.G., Almeida, V.C., 2011. Naoh-activated carbon of high surface area produced from coconut shell: Kinetics and equilibrium studies from the methylene blue adsorption. Chem. Eng. J. 174 (1), 117–125. http://dx.doi.org/10.1016/j.cej.2011.08.058.

Cheng, W.H., Zhan, W., Pawliszyn, J., 2013. Gaseous and particle-bound VOC products of combustion extracted by needle trap samplers. J. Chin. Chem. Soc. 60 (8), 1027–1032. http://dx.doi.org/10.1002/jccs.201200654.

De Schrijver, A., Staelens, J., Wuyts, K., Hoydonck, G.Van., Janssen, N., Mertens, J., Gielis, L., Geudens, G., Augusto, L., Verheyen, K., 2008. Effect of vegetation type on throughfall deposition and seepage flux. Environ. Pollut. 153 (2), 295–303. http://dx.doi.org/10.1016/j.envpol.2007.08.025.

Dehghani, M., Fazlzadeh, M., Sorooshian, A., Tabatabaee, H.R., Miri, M., Baghani, A.N., Delikhoon, M., Mahvi, A.M., Rashidi, M., 2018. Characteristics and health effects of BTEX in a hot spot for urban pollution. Ecotoxicol. Environ. Saf. 155, 133–143. http://dx.doi.org/10.1016/j.ecoenv.2018.02.065.

Dobre, T., Pârvulescu, O.C., Iavorschi, G., Stroescu, M., Stoica, A., 2014. Volatile organic compounds removal from gas streams by adsorption onto activated carbon. Ind. Eng. Chem. Res. 53 (9), 3622–3628. http://dx.doi.org/10.1021/ie402504u.

El Mohajir, A., Castro-Gutierrez, J., Canevesi, R.L.S., Bezverkhyy, I., Weber, G., Bellat, J.P., Berger, F., Celzard, A., Fierro, V., Sanchez, J.B., 2021. Novel porous carbon material for the detection of traces of volatile organic compounds in indoor air. ACS Appl. Mater. Interfaces 13 (33), 40088–40097. http://dx.doi.org/10.1021/acsami.1c10430.

Fang, L., Norris, C., Johnson, K., Cui, X., Sun, J., Teng, Y., Tian, E., Xu, W., Li, Z., Mo, J., Schauer, J.J., Black, M., Mike, Bergin., Zhang, J., Zhang, Y., 2019. Toxic volatile organic compounds in 20 homes in shanghai: Concentrations, inhalation health risks, and the impacts of household air cleaning. Build. Environ. 157, 309–318. http://dx.doi.org/10.1016/j.buildenv.2019.04.047.

Gaurh, P., Pramanik, H., 2018. Production of benzene/toluene/ethyl benzene/xylene (BTEX) via multiphase catalytic pyrolysis of hazardous waste polyethylene using low cost fly ash synthesized natural catalyst. Waste Manage. 77, 114–130. http://dx.doi.org/10.1016/j.wasman.2018.05.013.

Giraudet, S., Boulinguiez, B., Cloirec, P.Le., 2014. Adsorption and electrothermal desorption of volatile organic compounds and siloxanes onto an activated carbon fiber cloth for biogas purification. Energy Fuels 28 (6), 3924–3932. http://dx.doi.org/10.1021/ef500600b.

González-García, P., Centeno, T.A., Urones-Garrote, E., Ávila-Brande, D., Otero-Díaz, L.C., 2013. Microstructure and surface properties of lignocellulosic-based activated carbons. Appl. Surf. Sci. 265, 731–737. http://dx.doi.org/10.1016/j.apsusc.2012.11.092.

Guo, Y., Tan, C., Sun, J., Li, W., Zhang, J., Zhao, C., 2020. Porous activated carbons derived from waste sugarcane bagasse for CO2 adsorption. Chem. Eng. J. 381, 122736. http://dx.doi.org/10.1016/j.cej.2019.122736.

Hafner, S.D., Howard, C., Muck, R.E., Franco, R.B., Montes, F., Green, P.G., Mitloehner, F., Trabue, S.L., Rotz, C.A., 2013. Emission of volatile organic compounds from silage: Compounds, sources, and implications. Atmos. Environ. 77, 827–839. http://dx.doi.org/10.1016/j.atmosenv.2013.04.076.

Healy, R.M., Wang, J.M., Karellas, N.S., Todd, A., Sofowote, U., Su, Y., Munoz, A., 2019. Assessment of a passive sampling method and two online gas chromatographs for the measurement of benzene, toluene, ethylbenzene and xylenes in ambient air at a highway site. Atmos. Pollut. Res. 10 (4), 1123–1127. http://dx.doi.org/10.1016/j.apr.2019.01.017.

Isinkaralar, K., 2022a. High-efficiency removal of benzene vapor using activated carbon from althaea officinalis l. biomass as a lignocellulosic precursor. Environ. Sci. Pollut. Res. 29 (44), 66728–66740. http://dx.doi.org/10.1007/s11356-022-20579-2.

Isinkaralar, K., 2022b. Theoretical removal study of gas BTEX onto activated carbon produced from digitalis purpurea l. biomass. Biomass Convers. Biorefinery 12 (9), 4171–4181. http://dx.doi.org/10.1007/s13399-022-02558-2.

Isinkaralar, K., 2023a. Experimental evaluation of benzene adsorption in the gas phase using activated carbon from waste biomass. Biomass Convers. Biorefinery 1–10. http://dx.doi.org/10.1007/s13399-023-03979-3.

Isinkaralar, K., 2023b. A study on the gaseous benzene removal based on adsorption onto the cost-effective and environmentally friendly adsorbent. Molecules 28 (8), 3453. http://dx.doi.org/10.3390/molecules28083453.

Isinkaralar, K., Gullu, G., Turkyilmaz, A., 2022a. Experimental study of formaldehyde and BTEX adsorption onto activated carbon from lignocellulosic biomass. Biomass Convers. Biorefinery 1–11. http://dx.doi.org/10.1007/s13399-021-02287-y.

Isinkaralar, K., Gullu, G., Turkyilmaz, A., Dogan, M., Turhan, O., 2022b. Activated carbon production from horse chestnut shells for hydrogen storage. Int. J. Glob. Warming 26 (4), 361–373. http://dx.doi.org/10.1504/IJGW.2022.122430.

Isinkaralar, K., Meruyert, K., 2023. Adsorption behavior of multi-component BTEX on the synthesized green adsorbents derived from abelmoschus esculentus l. Waste residue. Appl. Biochem. Biotechnol. 1–17. http://dx.doi.org/10.1007/s12010-023-04556-0.

Isinkaralar, K., Turkyilmaz, A., 2022. Simultaneous adsorption of selected VOCs in the gas environment by low-cost adsorbent from ricinus communis. Carbon Lett. 32, 1781–1789. http://dx.doi.org/10.1007/s42823-022-00399-7.

Isinkaralar, O., Varol, C., 2023. A Cellular Automata-Based Approach for Spatio-Temporal Modeling of the City Center As a Complex System: The Case of Kastamonu. 132, 104073. http://dx.doi.org/10.1016/j.cities.2022.104073.

Jafari, A.J., Asl, Y.A., Momeniha, F., 2020. Determination of metals and BTEX in different components of waterpipe: charcoal, tobacco, smoke and water. J. Environ. Health Sci. Eng. 18 (1), 243–251. http://dx.doi.org/10.1007/s40201-020-00459-y.

Jia, C., Yu, X., Masiak, W., 2012. Blood/air distribution of volatile organic compounds (VOCs) in a nationally representative sample. Sci. Total Environ. 419, 225–232. http://dx.doi.org/10.1016/j.scitotenv.2011.12.055.

Kang, S., Baginska, M., White, S.R., Sottos, N.R., 2015. Core–shell polymeric microcapsules with superior thermal and solvent stability. ACS Appl. Mater. Interfaces 7 (20), 10952–10956. http://dx.doi.org/10.1021/acsami.5b02169.

Kong, Z.Y., Mahmoud, A., Liu, S., Sunarso, J., 2018. A parametric study of different recycling configurations for the natural gas dehydration process via absorption using triethylene glycol. Process Integr. Optim. Sustain. 2 (4), 447–460. http://dx.doi.org/10.1007/s41660-018-0058-x.

Konggidinata, M.I., Chao, B., Lian, Q., Subramaniam, R., Zappi, M., Gang, D.D., 2017. Equilibrium, kinetic and thermodynamic studies for adsorption of BTEX onto ordered mesoporous carbon (OMC). J. Hard Mater. 336, 249–259. http://dx.doi.org/10.1016/j.jhazmat.2017.04.073.

Korologos, C.A., Philippopoulos, C.J., Poulopoulos, S.G., 2011. The effect of water presence on the photocatalytic oxidation of benzene, toluene, ethylbenzene and m-xylene in the gas-phase. Atmos. Environ. 45 (39), 7089–7095. http://dx.doi.org/10.1016/j.atmosenv.2011.09.038.

Kumar, A., Jena, H.M., 2016. Preparation and characterization of high surface area activated carbon from fox nut (euryale ferox) shell by chemical activation with H3po4. Results Phys. 6, 651–658. http://dx.doi.org/10.1016/j.rinp.2016.09.012.

Laokiat, L., Khemthong, P., Grisdanurak, N., Sreearunothai, P., Pattanasiriwisawa, W., Klysubun, W., 2012. Photocatalytic degradation of benzene, toluene, ethylbenzene, and xylene (BTEX) using transition metal-doped titanium dioxide immobilized on fiberglass cloth. Korean J. Chem. Eng. 29 (3), 377–383. http://dx.doi.org/10.1007/s11814-011-0179-1.

Laskar, I.I., Hashisho, Z., Phillips, J.H., Anderson, J.E., Nichols, M., 2019. Competitive adsorption equilibrium modeling of volatile organic compound (VOC) and water vapor onto activated carbon. Sep. Purif. Technol. 212, 632–640. http://dx.doi.org/10.1016/j.seppur.2018.11.073.

Latif, M.T., Abd Hamid, H.H., Ahamad, F., Khan, M.F., Nadzir, M.S.M., Othman, M., Sahani, M., Wahab, M.I.A., Mohamad, N., Uning, R., Poh, S.C., Fadzil, M.F., Sentian, J., Tahir, N.M., 2019. BTEX compositions and its potential health impacts in Malaysia. Chemosphere 237, 124451. http://dx.doi.org/10.1016/j.chemosphere.2019.124451.

Li, X., Zhang, L., Yang, Z., Wang, P., Yan, Y., Ran, J., 2020. Adsorption materials for volatile organic compounds (VOCs) and the key factors for VOCs adsorption process: A review. Sep. Purif. Technol. 235, 116213. http://dx.doi.org/10.1016/j.seppur.2019.116213.

Liang, C., Li, C., Zhu, Y., Du, X., Yao, C., Ma, Y., Zhao, J., 2022. Recent advances of photocatalytic degradation for BTEX: Materials, operation, and mechanism. Chem. Eng. J. 140461. http://dx.doi.org/10.1016/j.cej.2022.140461.

Lim, S.K., Shin, H.S., Yoon, K.S., Kwack, S.J., Um, Y.M., Hyeon, J.H., Kwak, H.M., Kim, J.Y., Kim, T.H., Kim, Y.J., Roh, T.H., Lim, D.S., Shin, M.K., Choi, S.M., Kim, H.S., Lee, B.M., 2014. Risk assessment of volatile organic compounds benzene, toluene, ethylbenzene, and xylene (BTEX) in consumer products. J. Toxicol. Environ. Health A 77 (22–24), 1502–1521. http://dx.doi.org/10.1080/15287394.2014.955905.

Liu, Y.H., Hsi, H.C., Li, K.C., Hou, C.H., 2016. Electrodeposited manganese dioxide/activated carbon composite as a high-performance electrode material for capacitive deionization. ACS Sustain. Chem. Eng. 4 (9), 4762–4770. http://dx.doi.org/10.1021/acssuschemeng.6b00974.

Liu, Q., Liu, Y., Zhang, M., 2014. Source apportionment of personal exposure to carbonyl compounds and BTEX at homes in Beijing, China. Aerosol Air Qual. Res. 14 (1), 330–337. http://dx.doi.org/10.4209/aaqr.2013.01.0005.

Liu, R., Ma, S., Chen, D., Li, G., Yu, Y., Fan, R., An, T., 2022. Human exposure to BTEX emitted from a typical e-waste recycling industrial park: external and internal exposure levels, sources, and probabilistic risk implications. J. Hard Mater. 129343. http://dx.doi.org/10.1016/j.jhazmat.2022.129343.

Mahamad, M.N., Zaini, M.A.A., Zakaria, Z.A., 2015. Preparation and characterization of activated carbon from pineapple waste biomass for dye removal. Int. Biodeterioration Biodegrad. 102, 274–280. http://dx.doi.org/10.1016/j.ibiod.2015.03.009.

Martín-Benito, D., Cherubini, P., Río, M.Del., Cañellas, I., 2008. Growth response to climate and drought in pinus nigra arn. trees of different crown classes. Trees 22 (3), 363–373. http://dx.doi.org/10.1007/s00468-007-0191-6.

Meng, F., Song, M., Wei, Y., Wang, Y., 2019. The contribution of oxygen-containing functional groups to the gas-phase adsorption of volatile organic compounds with different polarities onto lignin-derived activated carbon fibers. Environ. Sci. Pollut. Res. 26 (7), 7195–7204. http://dx.doi.org/10.1007/s11356-019-04190-6.

Mikulová, K., Jarolímek, I., Bacigál, T., Hegedüšová, K., Májeková, J., Medvecká, J., Slabejová, D., Šibik, J., Škodavá, I., Zaliberová, M., Šibíková, M., 2019. The effect of non-native black pine (pinus nigra JF arnold) plantations on environmental conditions and undergrowth diversity. Forests 10 (7), 548. http://dx.doi.org/10.3390/f10070548.

Miller, L., Xu, X., Grgicak-Mannion, A., Brook, J., Wheeler, A., 2012. Multi-season, multi-year concentrations and correlations amongst the BTEX group of VOCs in an urbanized industrial city. Atmos. Environ. 61, 305–315. http://dx.doi.org/10.1016/j.atmosenv.2012.07.041.

Mistar, E.M., Alfatah, T., Supardan, M.D., 2020. Synthesis and characterization of activated carbon from bambusa vulgaris striata using two-step KOH activation. J. Mater. Res. Technol. 9 (3), 6278–6286. http://dx.doi.org/10.1016/j.jmrt.2020.03.041.

Morris, J.R., Contescu, C.I., Chisholm, M.F., Cooper, V.R., Guo, J., He, L., Ihm, Y., Mamontov, E., Melnichenko, Y.B., Olsen, R.J., Pennycook, S.J., Stone, M.B., Zhang, H., Gallego, N.C., 2013. Modern approaches to studying gas adsorption in nanoporous carbons. J. Mater. Chem. A 1 (33), 9341–9350. http://dx.doi.org/10.1039/C3TA10701A.

Najafi, A., Golestani-Fard, F., Rezaie, H.R., Ehsani, N., 2011. A study on sol–gel synthesis and characterization of SiC nano powder. J. Sol–Gel Sci. Technol. 59 (2), 205–214. http://dx.doi.org/10.1007/s10971-011-2482-z.

Nandanwar, S.U., Dantas, J., Coldsnow, K., Green, M., Utgikar, V., Sabharwall, P., Aston, D.E., 2016. Porous microsphere of magnesium oxide as an effective sorbent for removal of volatile iodine from off-gas stream. Adsorption 22 (3), 335–345. http://dx.doi.org/10.1007/s10450-016-9781-1.

Nayyeri, H., Ghanavati, H., Mazaheri, H., Joshaghani, A.H., 2022. Simultaneous biodegradation of BTX by isolated degrading bacterial strains in a newly designed modulated bio-scrubber assisted to airlift parallel bioreactors. J. Environ. Health Sci. Eng. 1–17. http://dx.doi.org/10.1007/s40201-021-00726-6.

Ogungbenro, A.E., Quang, D.V., Al-Ali, K.A., Vega, L.F., Abu-Zahra, M.R., 2018. Physical synthesis and characterization of activated carbon from date seeds for CO2 capture. J. Environ. Chem. Eng. 6 (4), 4245–4252. http://dx.doi.org/10.1016/j.jece.2018.06.030.

Ouzzine, M., Romero-Anaya, A.J., Lillo-Rodenas, M.A., Linares-Solano, A., 2019. Spherical activated carbons for the adsorption of a real multi-component VOC mixture. Carbon 148, 214–223. http://dx.doi.org/10.1016/j.carbon.2019.03.075.

Ovchinnikov, O.V., Evtukhova, A.V., Kondratenko, T.S., Smirnov, M.S., Khokhlov, V.Y., Erina, O.V., 2016. Manifestation of intermolecular interactions in FTIR spectra of methylene blue molecules. Vib. Spectrosc. 86, 181–189. http://dx.doi.org/10.1016/j.vibspec.2016.06.016.

Pallarés, J., González-Cencerrado, A., Arauzo, I., 2018. Production and characterization of activated carbon from barley straw by physical activation with carbon dioxide and steam. Biomass Bioenergy 115, 64–73. http://dx.doi.org/10.1016/j.biombioe.2018.04.015.

Paris, A., Gaillard, J.L., Ledauphin, J., 2020. Impact of biomass combustion on occurrence and distribution of aromatic hydrocarbons in apples. Environ. Sci. Pollut. Res. 27 (3), 3165–3172. http://dx.doi.org/10.1007/s11356-019-07228-x.

Pei, J., Yin, Y., Liu, J., 2016. Long-term indoor gas pollutant monitor of new dormitories with natural ventilation. Energy Build. 129, 514–523. http://dx.doi.org/10.1016/j.enbuild.2016.08.033.

Peng, H., Ma, G., Sun, K., Mu, J., Zhang, Z., Lei, Z., 2014. Formation of carbon nanosheets via simultaneous activation and catalytic carbonization of macroporous anion-exchange resin for supercapacitors application. ACS Appl. Mater. Interfaces 6 (23), 20795–20803. http://dx.doi.org/10.1021/am505066v.

Policicchio, A., Vuono, D., Rugiero, T., De Luca, P., Nagy, J.B., 2015. Study of MWCNTs adsorption performances in gas processes. J. CO2 Util. 10, 30–39. http://dx.doi.org/10.1016/j.jcou.2015.03.002.

Pontes-López, S., Moreno, J., Esteve-Turrillas, F.A., Armenta, S., 2020. Development of a simulation chamber for the evaluation of dermal absorption of volatile organic compounds. Atmos. Pollut. Res. 11 (5), 1009–1017. http://dx.doi.org/10.1016/j.apr.2020.02.015.

Rad, H.D., Babaei, A.A., Goudarzi, G., Angali, K.A., Ramezani, Z., Mohammadi, M.M., 2014. Levels and sources of BTEX in ambient air of ahvaz metropolitan city. Air Qual. Atmos. Health 7 (4), 515–524. http://dx.doi.org/10.1007/s11869-014-0254-y.

Rafiee, A., Delgado-Saborit, J.M., Sly, P.D., Amiri, H., Hoseini, M., 2019. Lifestyle and occupational factors affecting exposure to BTEX in municipal solid waste composting facility workers. Sci. Total Environ. 656, 540–546. http://dx.doi.org/10.1016/j.scitotenv.2018.11.398.

Rahimpoor, R., Firoozichahak, A., Nematollahi, D., Alizadeh, S., Alizadeh, P.M., Langari, A.A.A., 2021. Bio-monitoring of non-metabolized BTEX compounds in urine by dynamic headspace-needle trap device packed with 3D Ni/co-BTC bimetallic metal–organic framework as an efficient absorbent. Microchem. J. 166, 106229. http://dx.doi.org/10.1016/j.microc.2021.106229.

Rivett, M.O., Wealthall, G.P., Dearden, R.A., McAlary, T.A., 2011. Review of unsaturated-zone transport and attenuation of volatile organic compound (VOC) plumes leached from shallow source zones. J. Contam. Hydrol. 123 (3–4), 130–156. http://dx.doi.org/10.1016/j.jconhyd.2010.12.013.

Seifi, L., Torabian, A., Kazemian, H., Bidhendi, G.N., Azimi, A.A., Nazmara, S., AliMohammadi, M., 2011. Adsorption of BTEX on surfactant modified granulated natural zeolite nanoparticles: parameters optimizing by applying taguchi experimental design method. CLEAN–Soil, Air, Water 39 (10), 939–948. http://dx.doi.org/10.1002/clen.201000390.

Serafin, J., Ouzzine, M., Cruz Jr., O.F., Sreńscek-Nazzal, J., Gómez, I.C., Azar, F.Z., Mafull, C.A.R., Hotza, D., Rambo, C.R., 2021. Conversion of fruit waste-derived biomass to highly microporous activated carbon for enhanced CO2 capture. Waste Manage. 136, 273–282. http://dx.doi.org/10.1016/j.wasman.2021.10.025.

Shakeri, H., Arshadi, M., Salvacion, J.W.L., 2016. Removal of BTEX by using a surfactant–bio originated composite. J. Colloid Interface Sci. 466, 186–197. http://dx.doi.org/10.1016/j.jcis.2015.12.019.

Shen, Y., Zhang, N., 2019. Facile synthesis of porous carbons from silica-rich rice husk char for volatile organic compounds (VOCs) sorption. Bioresour. Technol. 282, 294–300. http://dx.doi.org/10.1016/j.biortech.2019.03.025.

Shi, X., Zhang, X., Bi, F., Zheng, Z., Sheng, L., Xu, J., Wang, Z., Yang, Y., 2020. Effective toluene adsorption over defective uio-66-NH2: An experimental and computational exploration. J. Mol. Liq. 316, 113812. http://dx.doi.org/10.1016/j.molliq.2020.113812.

Stähelin, P.M., Valério, A., Ulson, S.M.D.A.G., da Silva, A., Valle, J.A.B., de Souza, A.A.U., 2018. Benzene and toluene removal from synthetic automotive gasoline by mono and bicomponent adsorption process. Fuel 231, 45–52. http://dx.doi.org/10.1016/j.fuel.2018.04.169.

Sui, H., An, P., Li, X., Cong, S., He, L., 2017. Removal and recovery of o-xylene by silica gel using vacuum swing adsorption. Chem. Eng. J. 316, 232–242. http://dx.doi.org/10.1016/j.cej.2017.01.061.

Tamrakar, A., Pervez, S., Verma, M., Majumdar, D., Pervez, Y.F., Candeias, C., Dugga, P., Mishra, A., Verma, S.R., Deb, M.K., Shrivas, K., Satnami, M.L., Karbhal, I., 2022. BTEX in ambient air of India: a scoping review of their concentrations, sources, and impact. Water Air Soil Pollut. 233 (10), 1–19. http://dx.doi.org/10.1007/s11270-022-05863-8.

Torasso, N., González-Seligra, P., Trupp, F., Grondona, D., Goyanes, S., 2022. Turning a novel janus electrospun mat into an amphiphilic membrane with high aromatic hydrocarbon adsorption capacity. Colloids Interfaces 6 (4), 66. http://dx.doi.org/10.3390/colloids6040066.

Verma, V.K., Subbiah, S., Kota, S.H., 2019. Sericin-coated polyester based air-filter for removal of particulate matter and volatile organic compounds (BTEX) from indoor air. Chemosphere 237, 124462. http://dx.doi.org/10.1016/j.chemosphere.2019.124462.

Wang, H., Xiang, Z., Wang, L., Jing, S., Lou, S., Tao, S., Liu, J., Yu, M., Li, L., Lin, L., Chen, Y., Wiedensohler, A., Chen, C., 2018a. Emissions of volatile organic compounds (VOCs) from cooking and their speciation: A case study for shanghai with implications for China. Sci. Total Environ. 621, 1300–1309. http://dx.doi.org/10.1016/j.scitotenv.2017.10.098.

Wang, B., Xu, X., Xu, W., Wang, N., Xiao, H., Sun, Y., Huang, H., Yu, L., Fu, M., Wu, J., Chen, L., Ye, D., 2018b. The mechanism of non-thermal plasma catalysis on volatile organic compounds removal. Catal. Surv. from Asia 22, 73–94. http://dx.doi.org/10.1007/s10563-018-9241-x.

Yang, J., Roth, P., Durbin, T., Karavalakis, G., 2019. Impacts of gasoline aromatic and ethanol levels on the emissions from GDI vehicles: Part 1. Influence on regulated and gaseous toxic pollutants. Fuel 252, 799–811. http://dx.doi.org/10.1016/j.fuel.2019.04.143.

Zhang, X., Gao, B., Fang, J., Zou, W., Dong, L., Cao, C., Zhang, J., Li, Y., Wang, H., 2019. Chemically activated hydrochar as an effective adsorbent for volatile organic compounds (VOCs). Chemosphere 218, 680–686. http://dx.doi.org/10.1016/j.chemosphere.2018.11.144.

Zhou, X., Moghaddam, T.B., Chen, M., Wu, S., Adhikari, S., 2020. Biochar removes volatile organic compounds generated from asphalt. Sci. Total Environ. 745, 141096. http://dx.doi.org/10.1016/j.scitotenv.2020.141096.

Zubrik, A., Matik, M., Hredzák, S., Lovás, M., Danková, Z., Kováčová, M., Briančin, J., 2017. Preparation of chemically activated carbon from waste biomass by single-stage and two-stage pyrolysis. J. Clean. Prod. 143, 643–653. http://dx.doi.org/10.1016/j.jclepro.2016.12.061.